Supporting Materials

For

Reactivity of A Two-Coordinate Cobalt(0) Cyclic (Alkyl)(amino)carbene Complex

Jingzhen Du[†], Wenwei Chen[†], Qi Chen[†], Xuebing Leng[†], Yin-Shan Meng[‡], Song Gao[‡], and Liang Deng*[,†]

[†] State Key Laboratory of Organometallic Chemistry, Center for Excellence in Molecular Synthesis, Shanghai Institute of Organic Chemistry, University of Chinese Academy of Sciences, Chinese Academy of Sciences, 345 Lingling Road, Shanghai 200032, P. R. China.

[‡] Beijing National Laboratory for Molecular Sciences, State Key Laboratory of Rare Earth Materials Chemistry and Applications, College of Chemistry and Molecular Engineering, Peking University, Beijing, 100871, P. R. China.

E-mail: deng@sioc.ac.cn

Table of Contents

Table S1. Key Distances (Å), Angles (°) and Solution Magnetic Moments (μB) of **2**, [(Et_2-cAAC)$_2$Co](**2'**), **4**, and [(Et_2-cAAC)$_2$Co][$BAr^F{}_4$](**4'**)

	2	**2'**	**4a**	**4b**	**4'**
C1-N1	1.352(5)	1.355(5)	1.300(4)	1.301(4)	1.308(3)
C2-N2	1.343(5)	1.358(5)	1.300(4)	1.301(4)	1.313(3)
C1-Co	1.868(4)	1.882(4)	1.944(3)	1.951(4)	1.957(2)
C2-Co	1.872(4)	1.875(4)	1.944(3)	1.951(4)	1.957(2)
C1-Co-C2	170.66(18)	170.48(18)	180.00(8)	180.00(8)	168.35(9)
α	71.11	68.19	0.00	0.00	55.95
μ_{eff}	3.7(1)	2.0	4.8(1)	4.8(1)	3.2

Data for **2'** and **4'** is extracted from ref. 1. **4a** and **4b** are two crystallographically independent molecules in the asymmetric unit. α Dihedral angles between the two central plane of R_2-cAAC, R = Me, Et.

Ref. 1: Ung, G.; Rittle, J.; Soleilhavoup, M.; Bertrand, G.; Peters, J. C. Two-Coordinate Fe^o and Co^o Complexes Supported by Cyclic (alkyl)(amino)carbenes. *Angew. Chem., Int. Ed.* **2014**, *53*, 8427–8431.

Table S2. X-ray Crystallography Data for **1** – **4**.

Compound	**1**	**2**	**3**	**4•Et$_2$O**
formula	$C_{40}H_{62}ClCoN_2$	$C_{40}H_{62}CoN_2$	$C_{40}H_{62}BrCoN_2$	$C_{76}H_{84}BCoF_{24}N_2O$
crystal size (mm^3)	0.16 x 0.12 x 0.08	0.25 x 0.22 x 0.16	0.22 x 0.16 x 0.12	0.25 x 0.22 x 0.20
fw	665.30	629.85	709.75	1567.19
crystal system	monoclinic	triclinic	monoclinic	triclinic
space group	*P 21/c*	*P-1*	*P 21/c*	*P-1*
a, Å	11.1897(17)	9.122(5)	11.2075(6)	12.7124(12)
b, Å	19.458(3)	12.200(6)	19.4931(10)	13.0186(13)
c, Å	16.905(3)	18.008(10)	16.9336(9)	24.968(3)
α, deg	90	82.291(10)	90	93.374(2)
β, deg	97.299(3)	76.953(10)	97.3880(10)	102.425(2)
γ, deg	90	87.823(9)	90	109.126(2)
V, Å^3	3650.8(10)	1934.5(18)	3668.8(3)	3774.9(6)
Z	4	2	4	2
D_{calcd}, Mg/m^3	1.210	1.081	1.285	1.379
radiation (λ), Å	Mo Kα (0.71073)	Mo Kα (0.71073)	Mo Kα (0.71073)	Mo Kα (0.71073)
2θ range, deg	3.200 to 61.340	2.340 to 52.000	3.664 to 61.182	1.686 to 52.000
μ, mm^{-1}	0.573	0.470	1.586	0.331
F(000)	1440	686	1512	1620
no. of obsd reflns	35946	14337	36940	27777
no. of params refnd	413	404	413	1021
goodness of fit	1.003	0.933	1.016	1.024
R1	0.0579	0.0766	0.0351	0.0633
*w*R2	0.1242	0.1709	0.0841	0.1466

Table S3. X-ray Crystallography Data for **6**, **7**, and **9**.

Compound	**6**	**7**	**9**
formula	$C_{65}H_{88}CoN_4$	$C_{47}H_{58}CoN_4$	$C_{46}H_{72}CoN_2$
crystal size (mm^3)	0.33 x 0.11 x 0.05	0.20 x 0.15 x 0.18	0.25 x 0.20 x 0.08
fw	984.32	737.90	711.98
crystal system	orthorhombic	monoclinic	monoclinic
space group	*P b c a*	*P 21/c*	*C 2/c*
a, Å	23.095(2)	20.407(3)	20.4464(17)
b, Å	18.2606(17)	11.0093(19)	10.9375(9)
c, Å	27.518(3)	18.572(3)	18.8522(16)
α, deg	90	90	90
β, deg	90	96.869(3)	99.648(2)
γ, deg	90	90	90
V, $Å^3$	11605.1(19)	4142.5(12)	4156.3(6)
Z	8	4	4
D_{calcd}, Mg/m^3	1.127	1.183	1.138
radiation (λ), Å	Mo Kα (0.71073)	Mo Kα (0.71073)	Mo Kα (0.71073)
2θ range, deg	2.960 to 52.000	2.010 to 50.604	4.042 to 52.000
μ, mm^{-1}	0.337	0.450	0.445
F(000)	4264	1580	1556
no. of obsd reflns	81409	7511	14856
no. of params refnd	653	484	231
goodness of fit	0.996	1.116	0.993
R1	0.0486	0.0759	0.0541
*w*R2	0.1025	0.200	0.1435

Table S4. Relative Energies of **6** and **9** at Their Doublet and Quartet States

	$S = 1/2$ (kcal/mol)	$S = 3/2$ (kcal/mol)
6[a]	0	32.2
9[b]	0	37.1

[a.] Calculation at the BP86 level of thoery. [b.] Calculation at the B3LYP level of theorey.

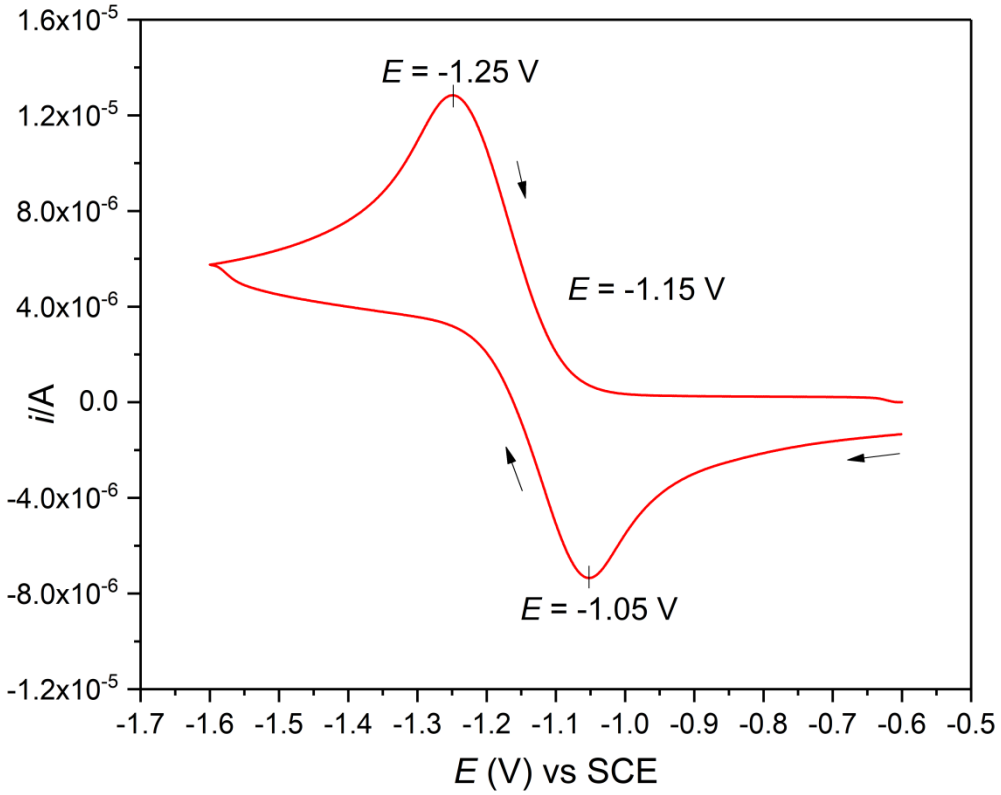

Figure S1. Cyclic voltammogram (100 mV/s) of **4** in THF, containing 0.1 M $^{n}Bu_4NPF_4$ as supporting electrolyte [$E_{1/2}$ = -1.15 V versus $(Cp_2Fe)/(Cp_2Fe)^+$].

Molecular Structures

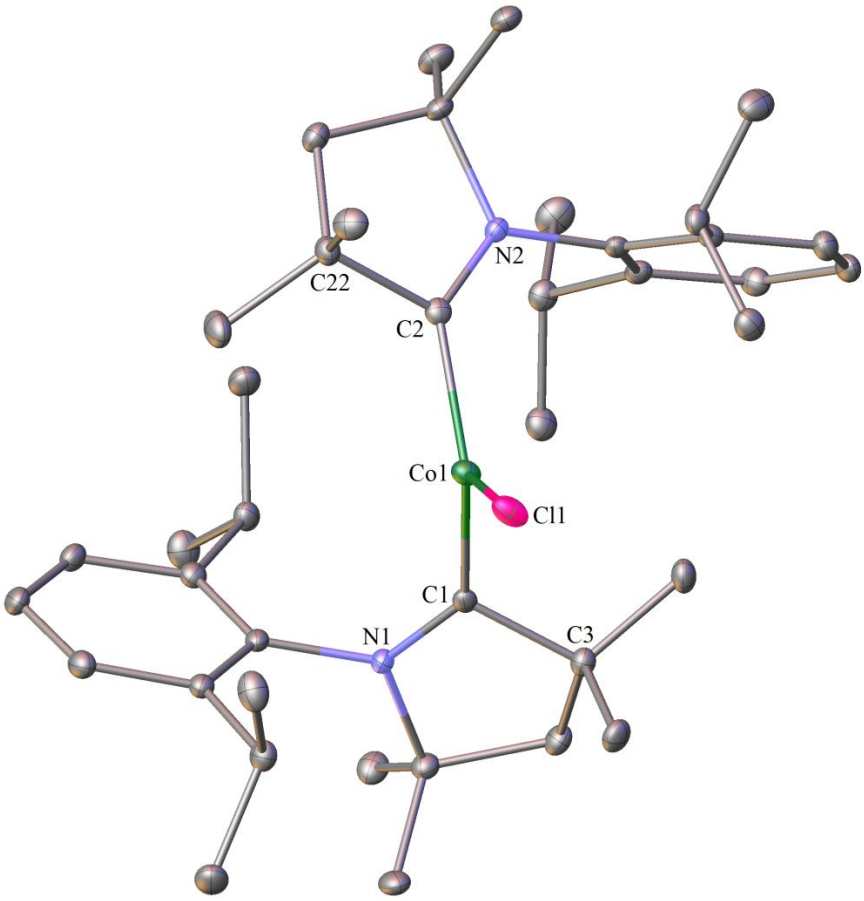

Figure S2. Molecular structure of **1**. Hydrogen atoms are omitted for clarity. Selected bond distances (Å) and angles (°): Co1-C1 1.936(3), Co1-C2 1.920(3), Co1-Cl1 2.2661(8), C1-N1 1.332(3), C2-N2 1.333(3), C1-C3 1.538(4), C2-C22 1.534(4), C1-Co1-C2 121.36(11), C1-Co1-Cl1 119.57(8), C2-Co1-Cl1 119.00(8).

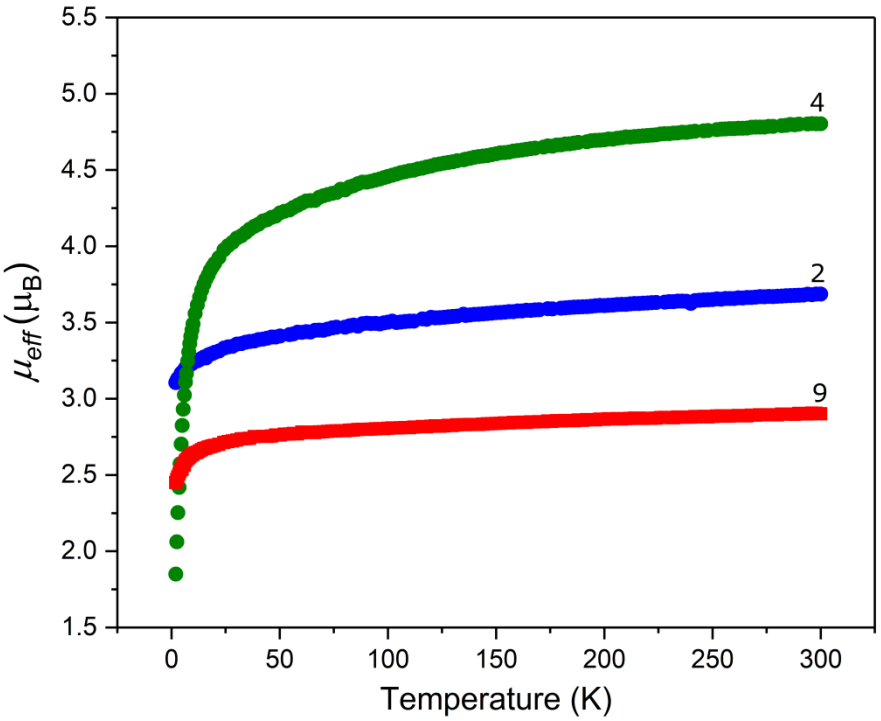

Figure S3. Variable temperature SQUID (superconducting quantum interference device) magnetic moment data for **2** (blue), **4** (green), and **9** (red) over the range 2 – 300 K. (These data were collected under a 1 kOe applied dc field).

UV-Vis-NIR Spectra

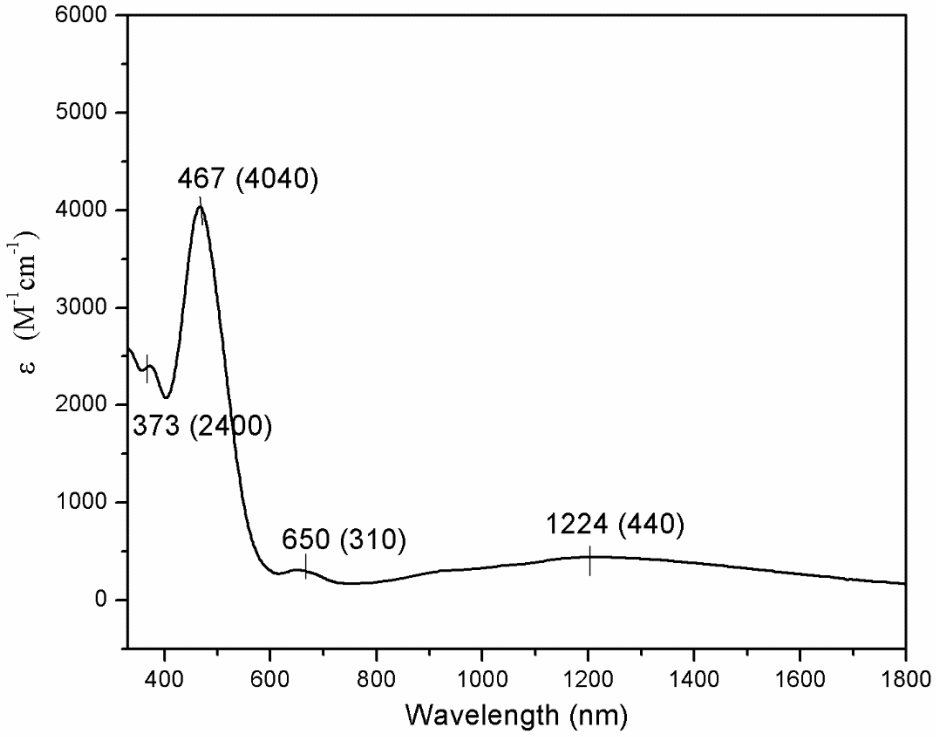

Figure S4. UV-Vis-NIR spectrum of **1** recorded at room temperature in THF.

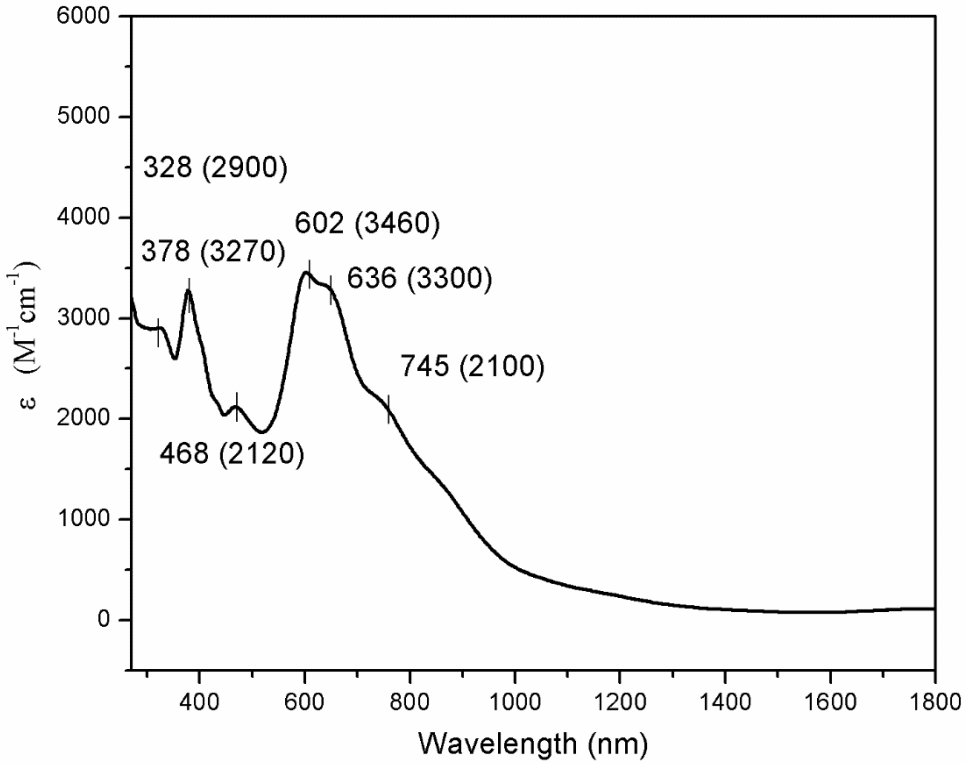

Figure S5. UV-Vis-NIR spectrum of **2** recorded at room temperature in THF.

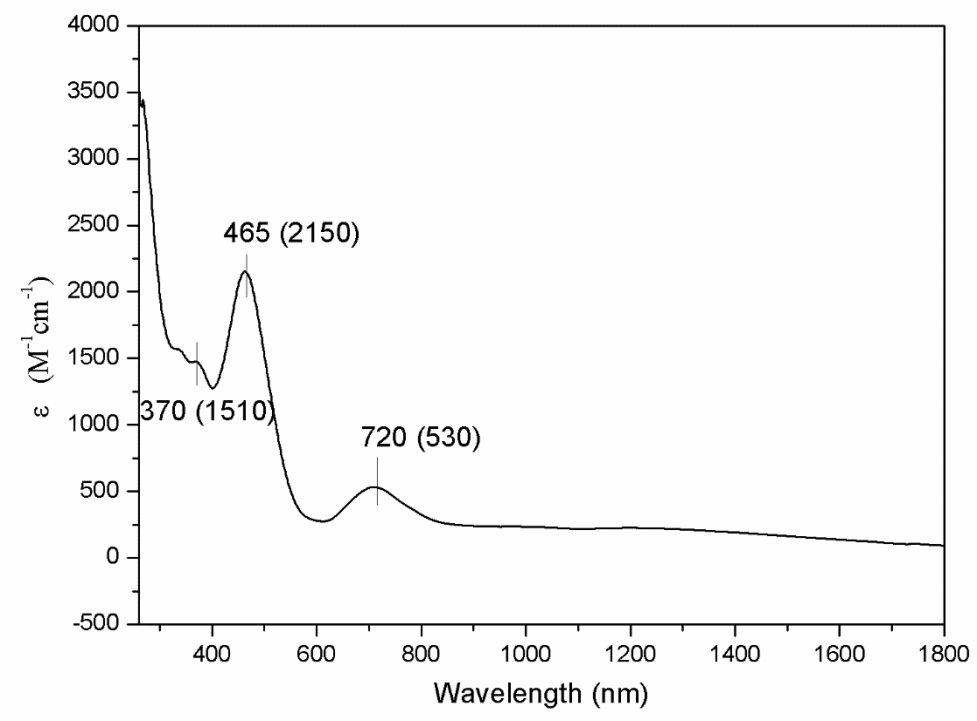

Figure S6. UV-Vis-NIR spectrum of **3** recorded at room temperature in THF.

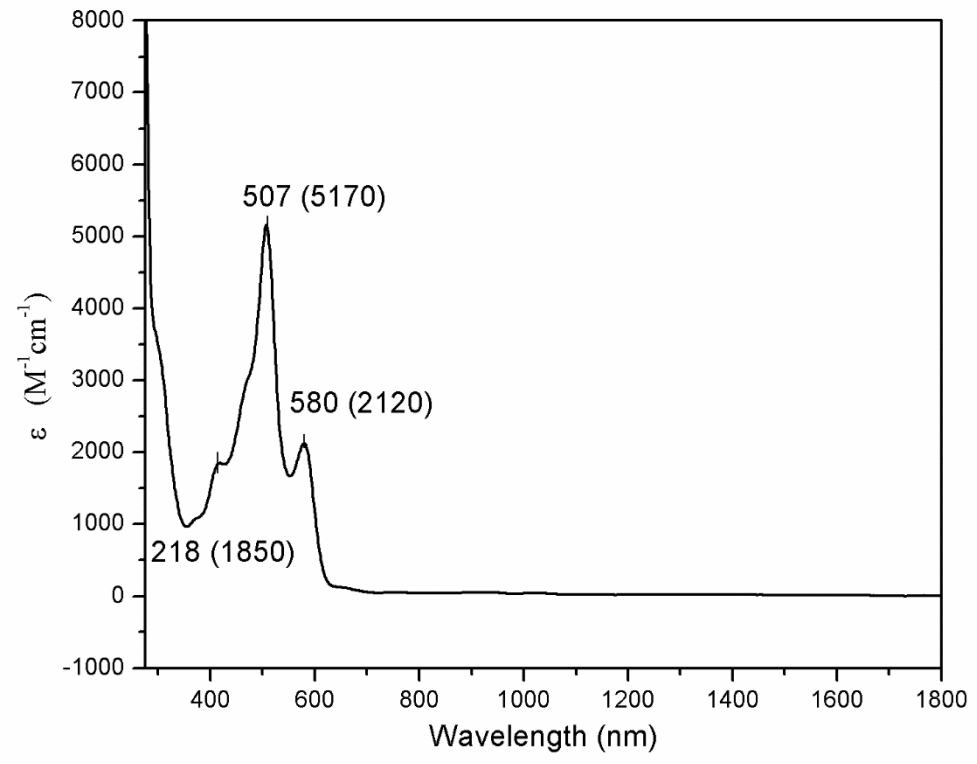

Figure S7. UV-Vis-NIR spectrum of **4** recorded at room temperature in THF.

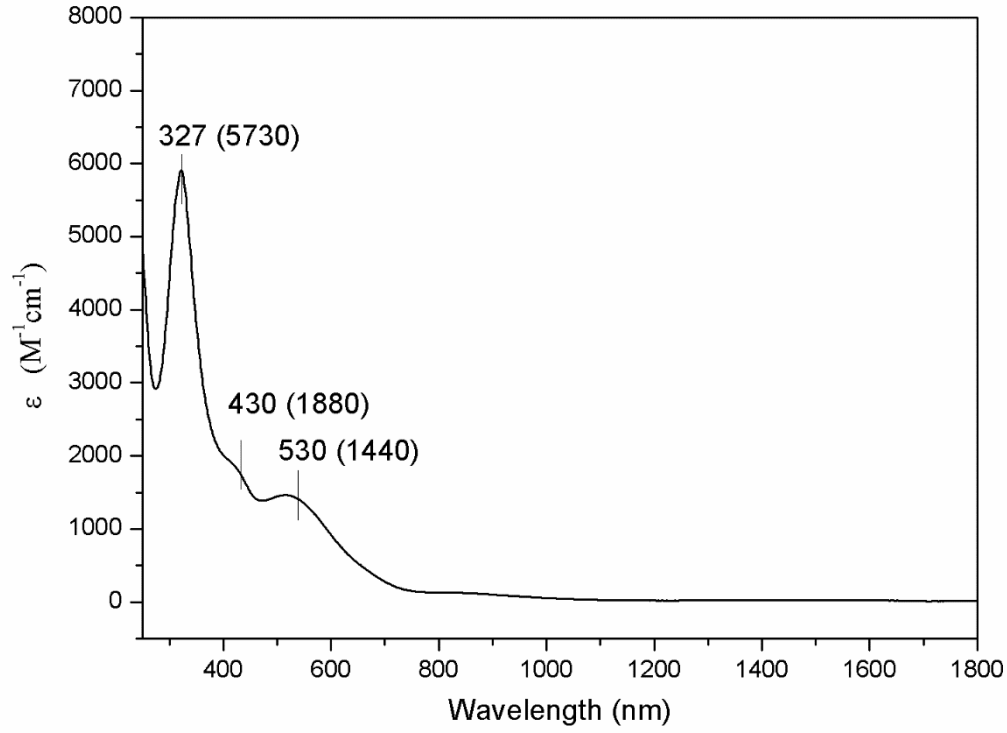

Figure S8. UV-Vis-NIR spectrum of **5** recorded at room temperature in benzene.

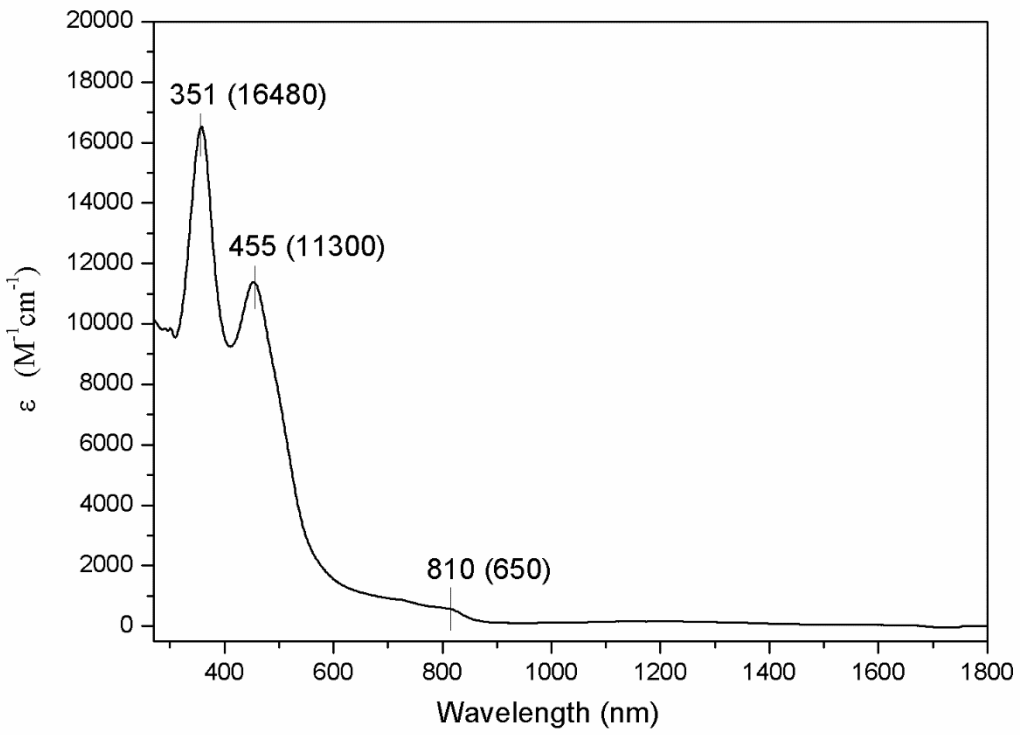

Figure S9. UV-Vis-NIR spectrum of **6** recorded at room temperature in benzene.

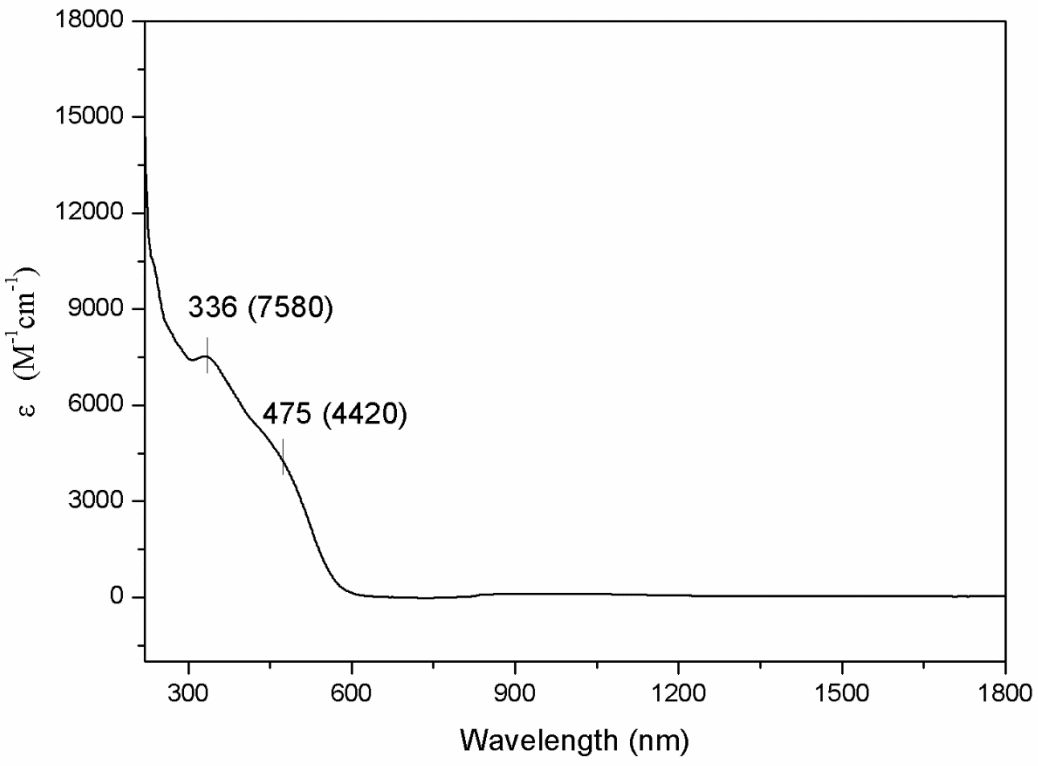

Figure S10. UV-Vis-NIR spectrum of **7** recorded at room temperature in benzene.

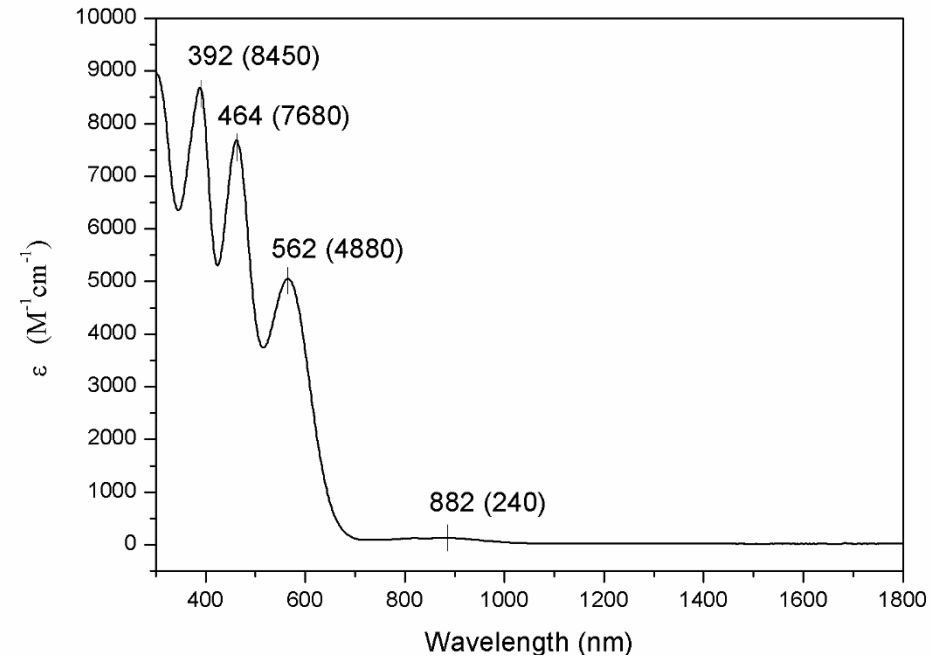

Figure S11. UV-Vis-NIR spectrum of **9** recorded at room temperature in benzene.

NMR Spectra

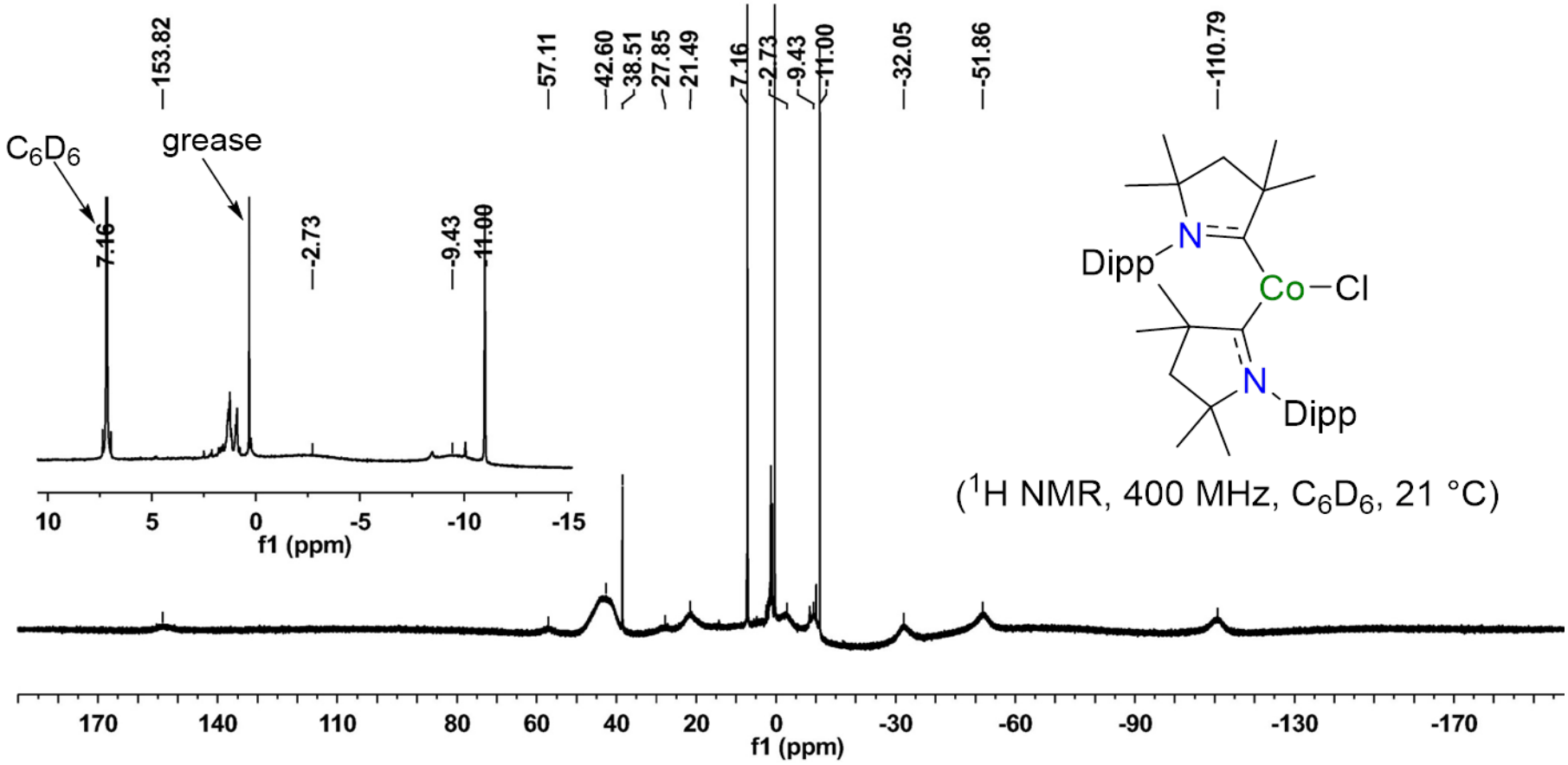

Figure S12. ^{1}H NMR spectrum for **1**.

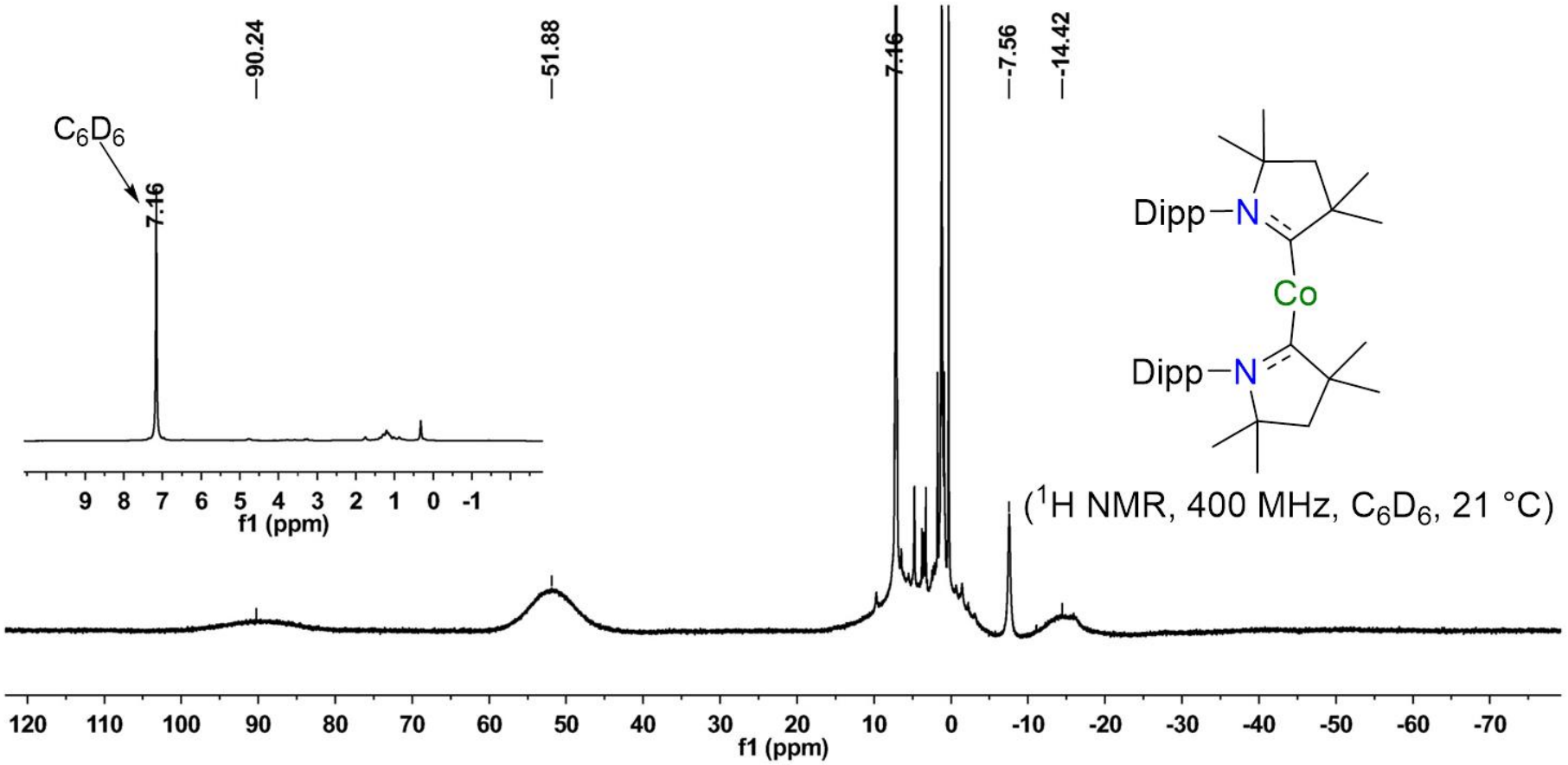

Figure S13. ^{1}H NMR spectrum for **2**.

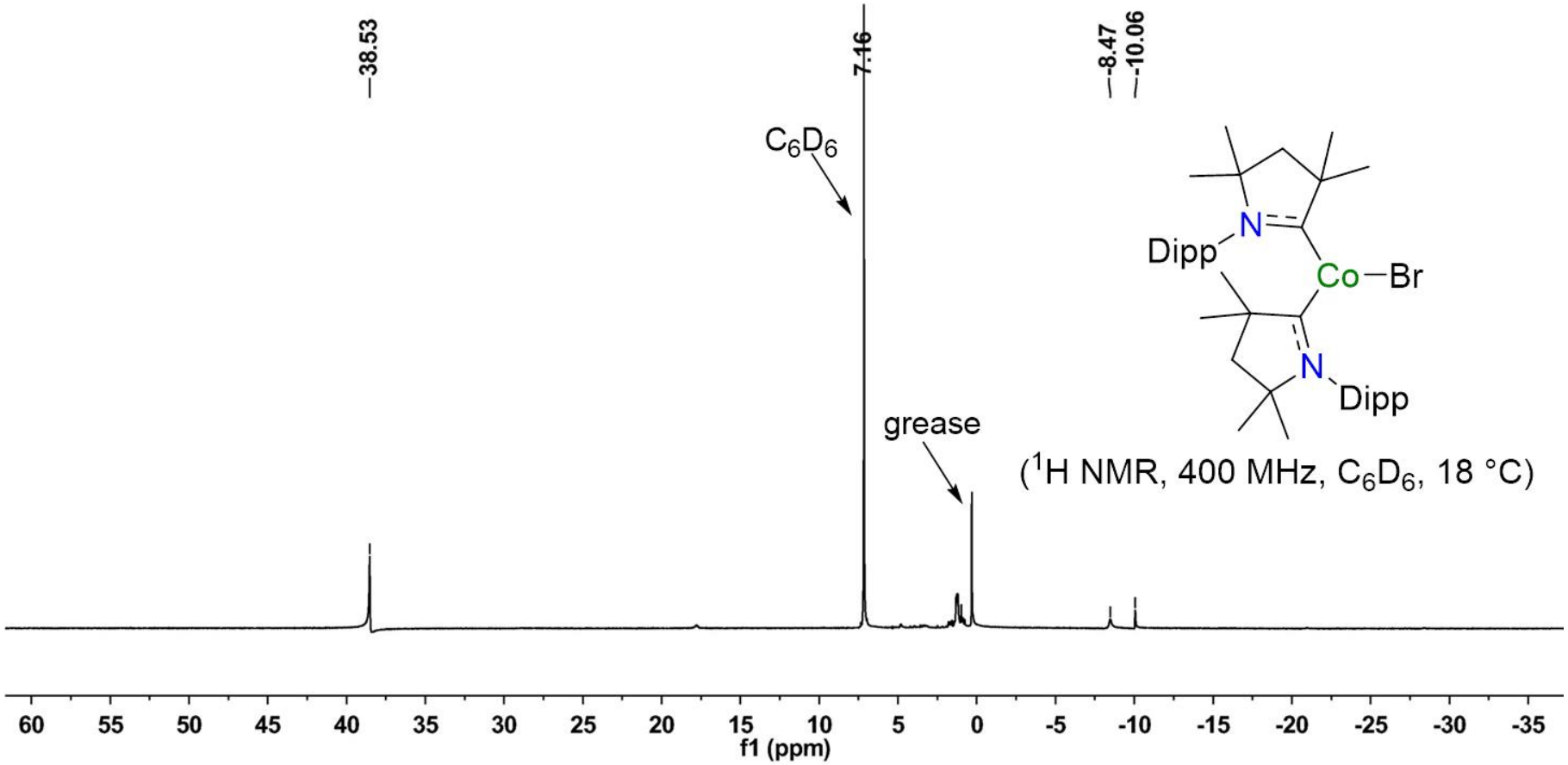

Figure S14. ^{1}H NMR spectrum for **3**.

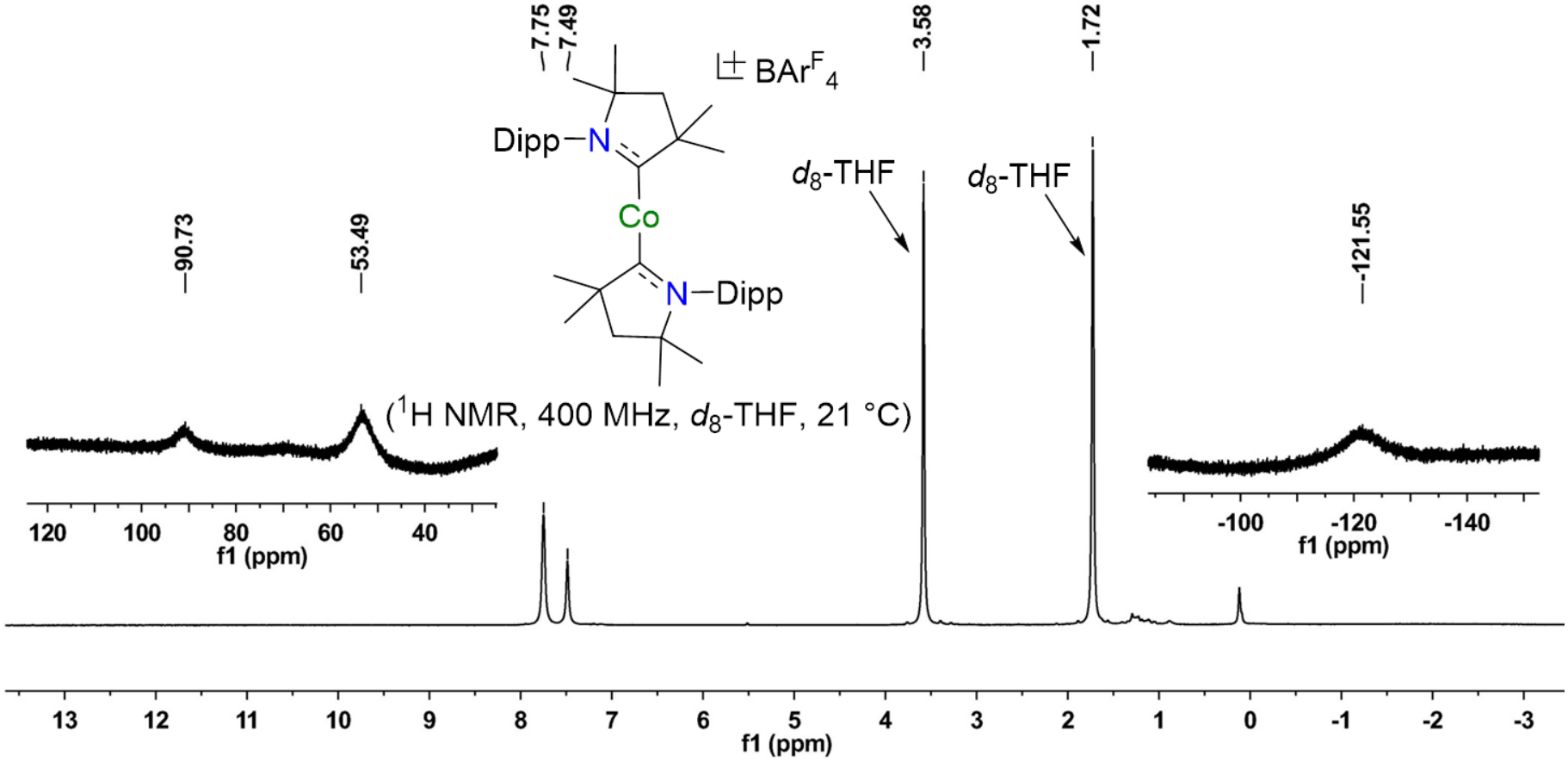

Figure S15. ^{1}H NMR spectrum for **4**.

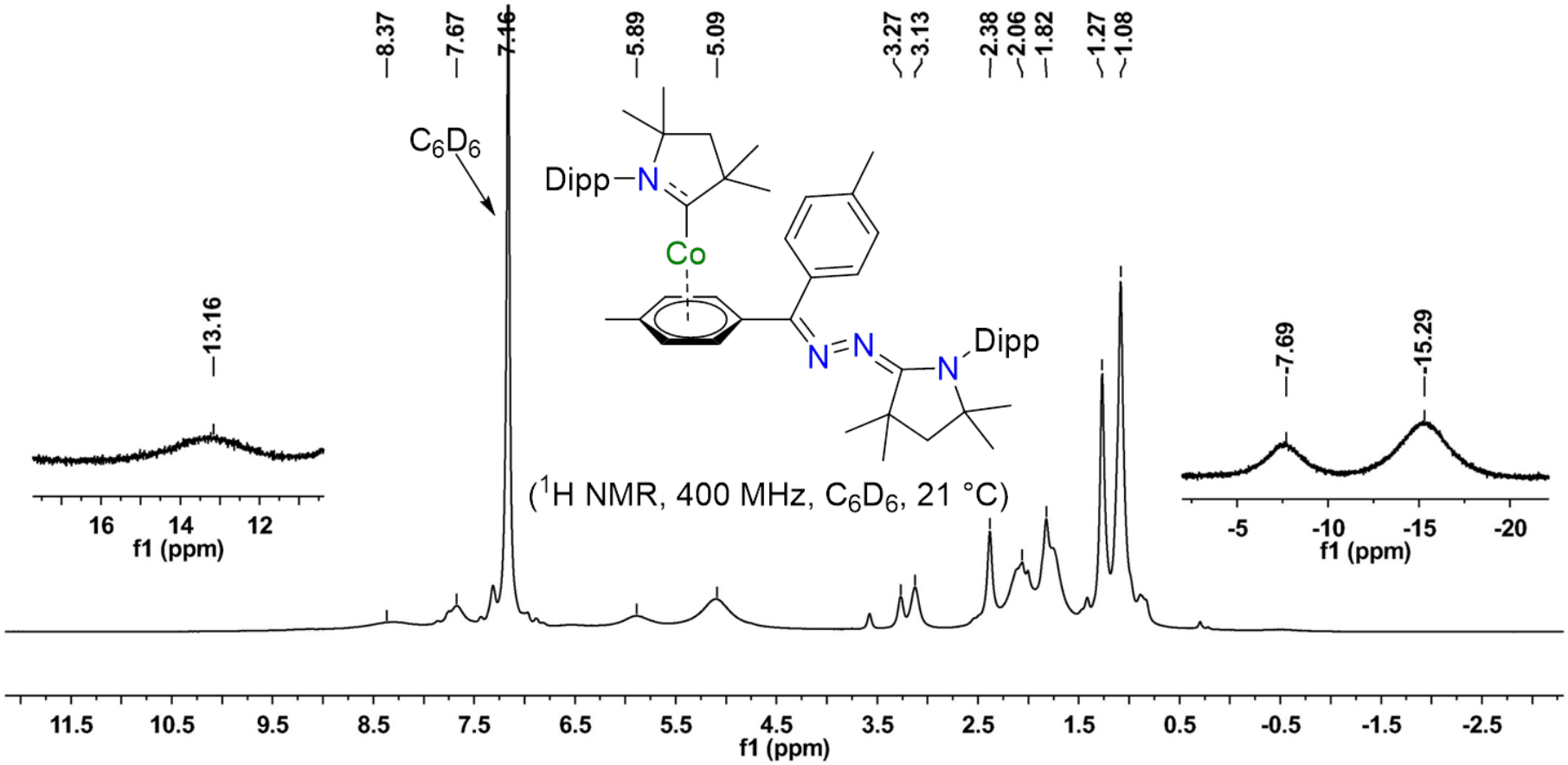

Figure S16. ^{1}H NMR spectrum for **5**.

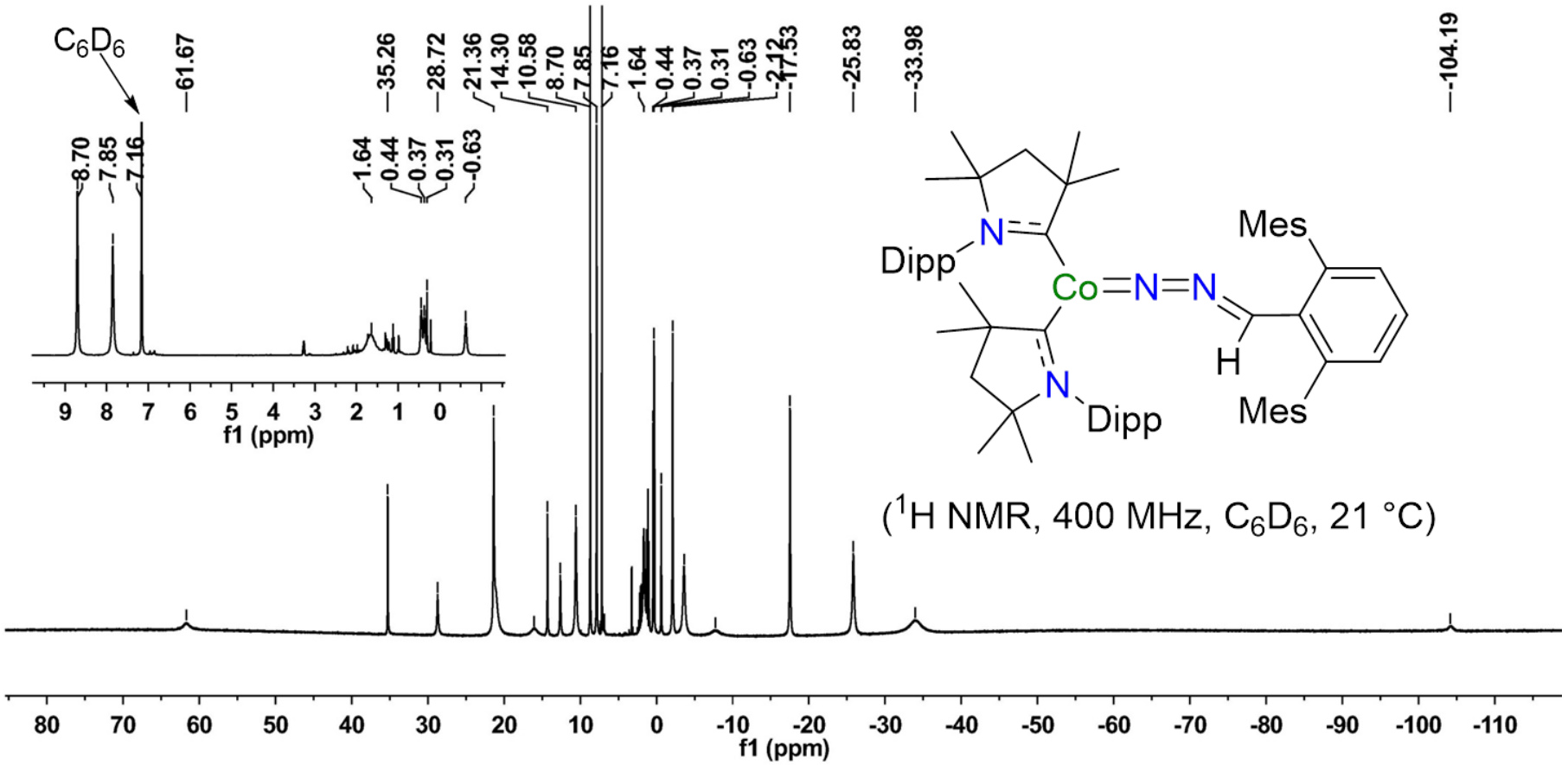

Figure S17. ^{1}H NMR spectrum for **6**.

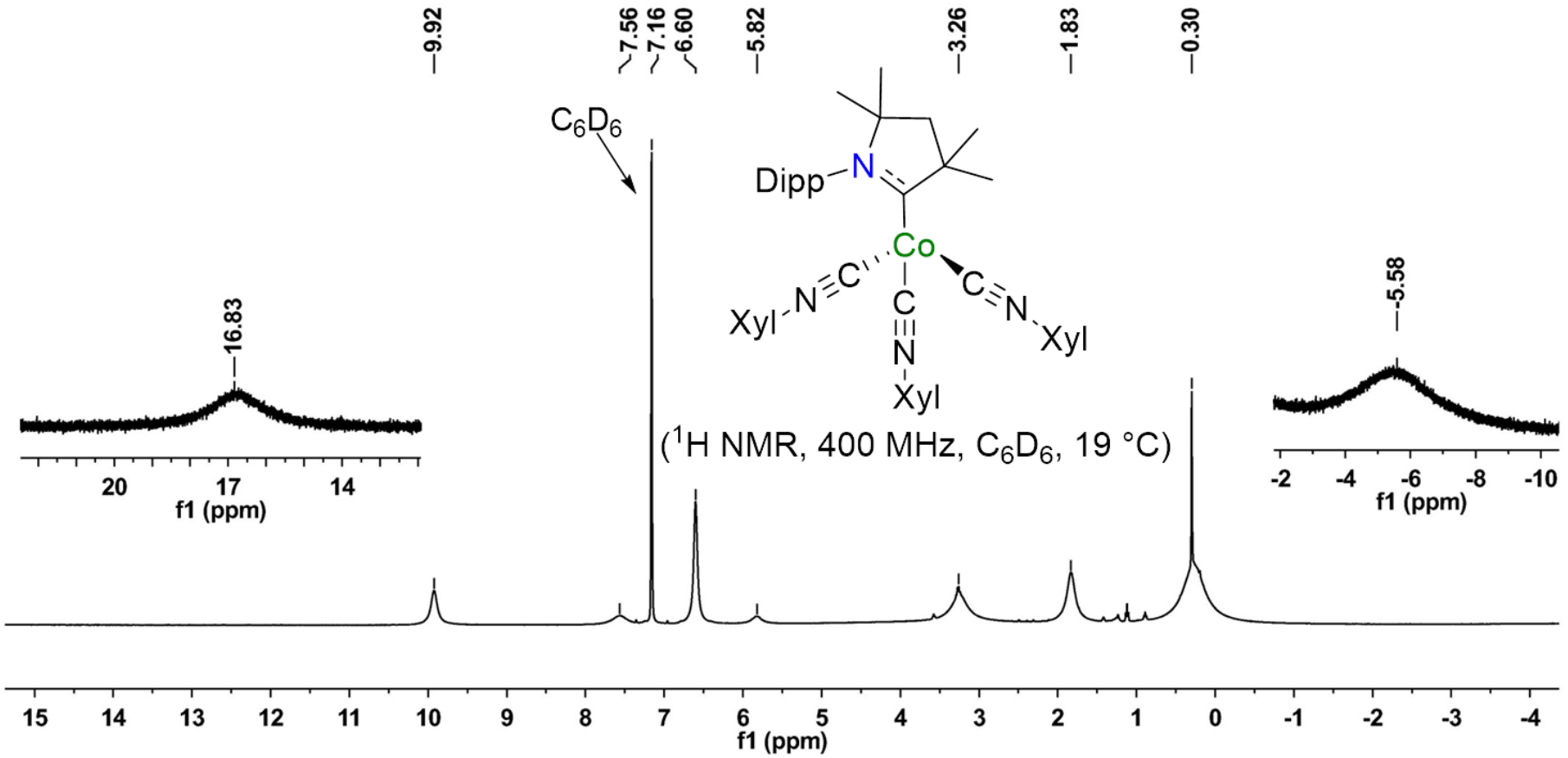

Figure S18. ^{1}H NMR spectrum for **7**.

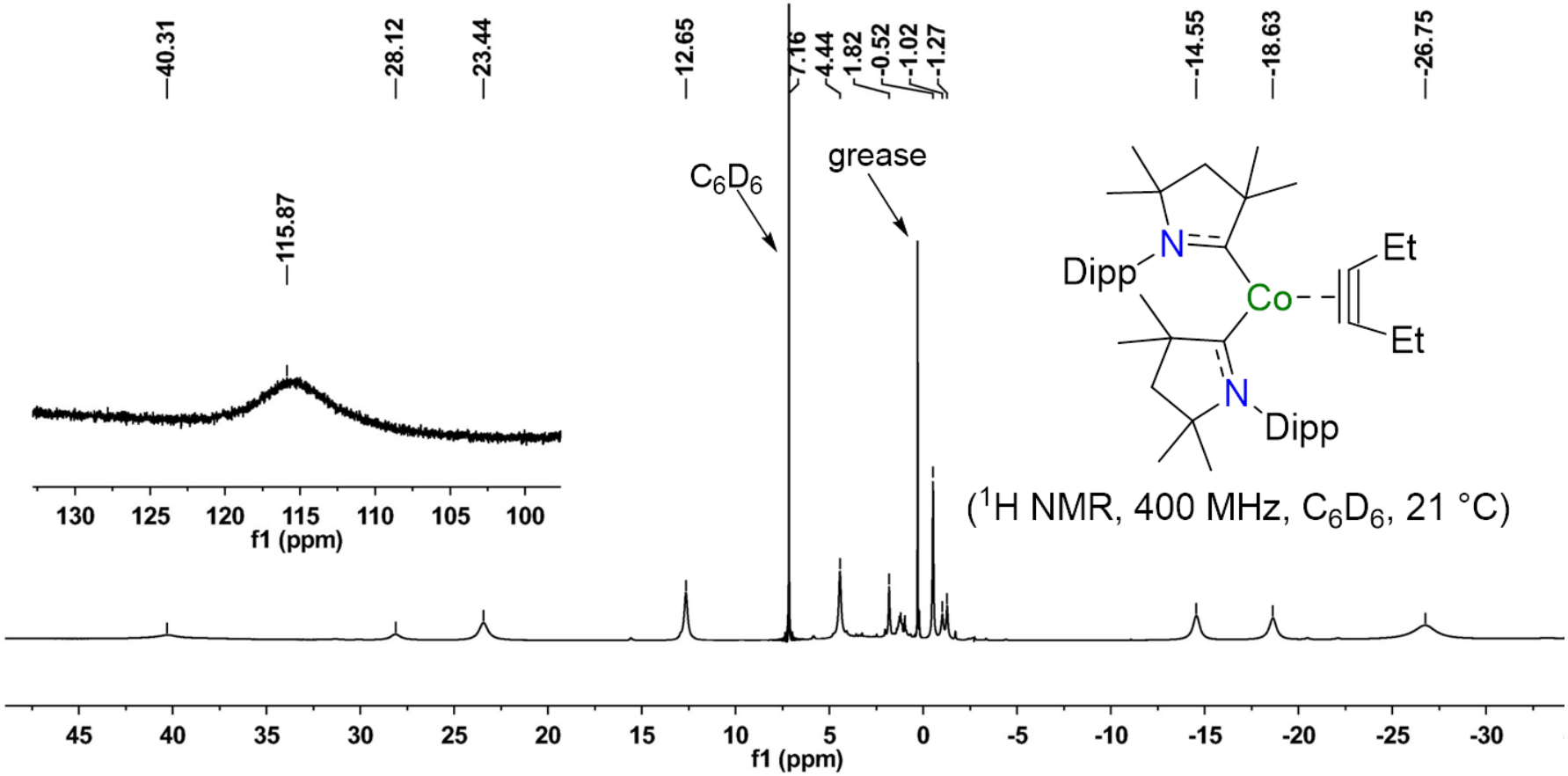

Figure S19. ^{1}H NMR spectrum for **9**.

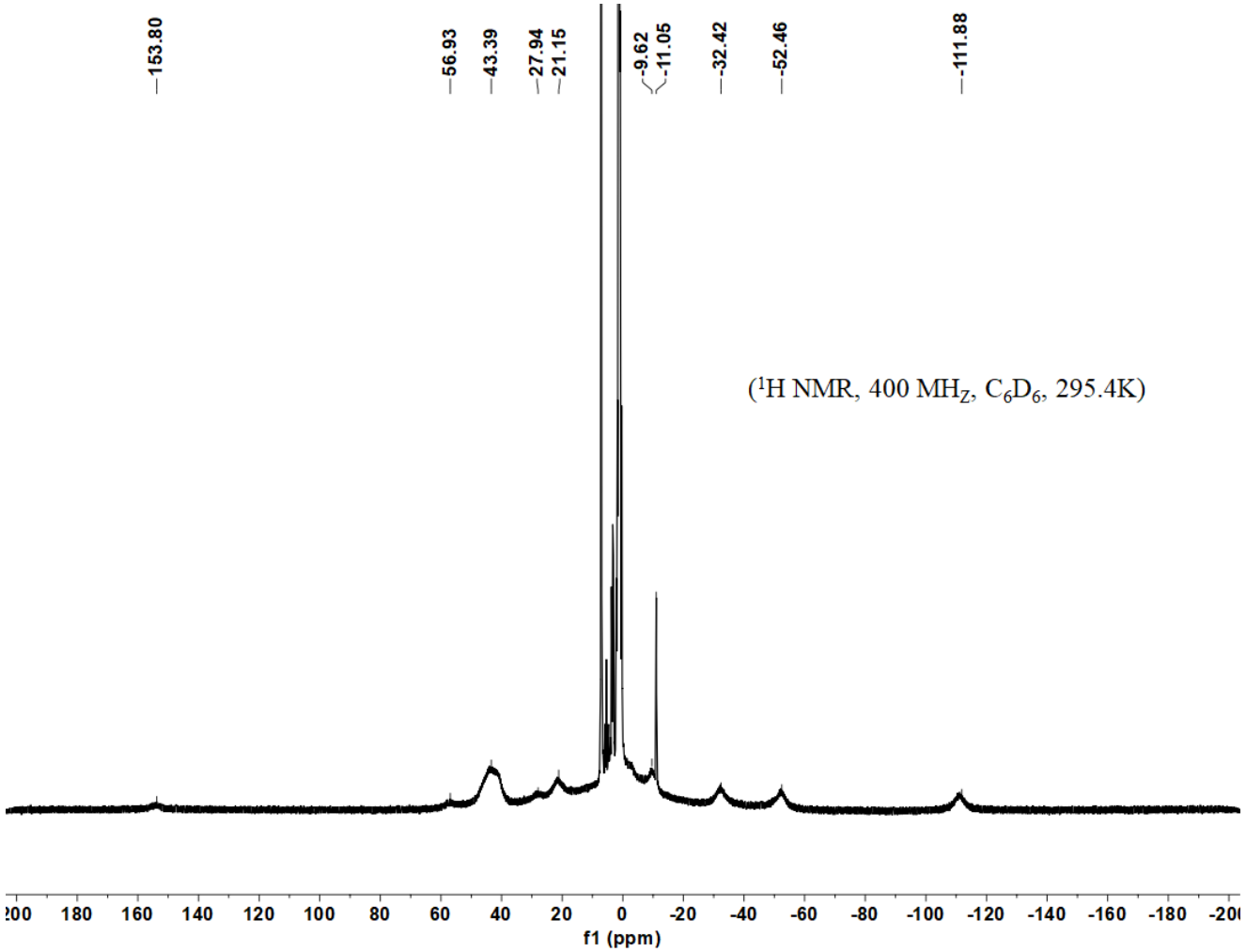

Figure S20. ^{1}H NMR spectrum for reaction of **2** with n-$C_8H_{17}Cl$.

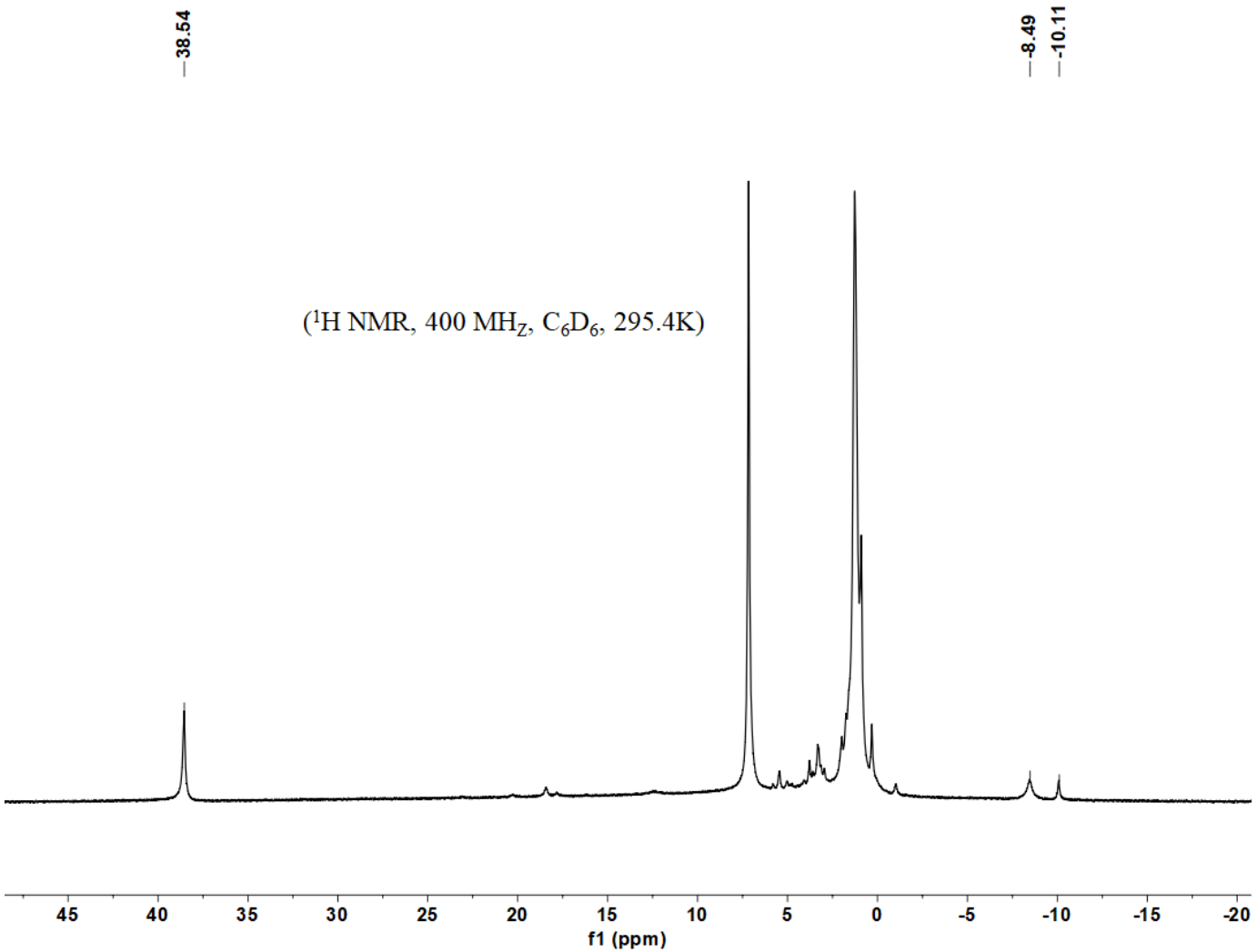

Figure S21. ^{1}H NMR spectrum for reaction of **2** with n-$C_8H_{17}Br$.

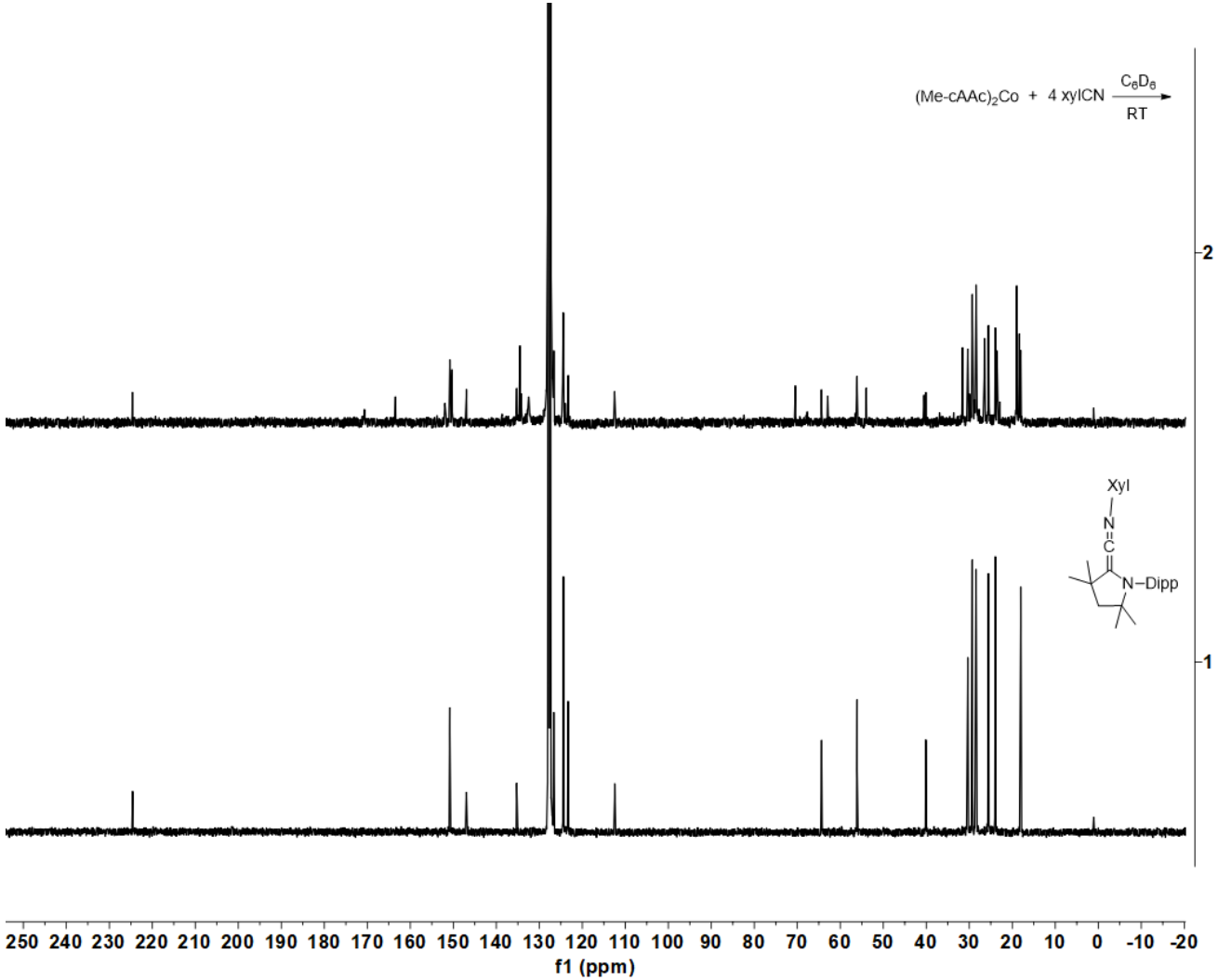

Figure S22. ^{13}C NMR spectrum for reaction of **2** with 2,6-Me_2PhNC.

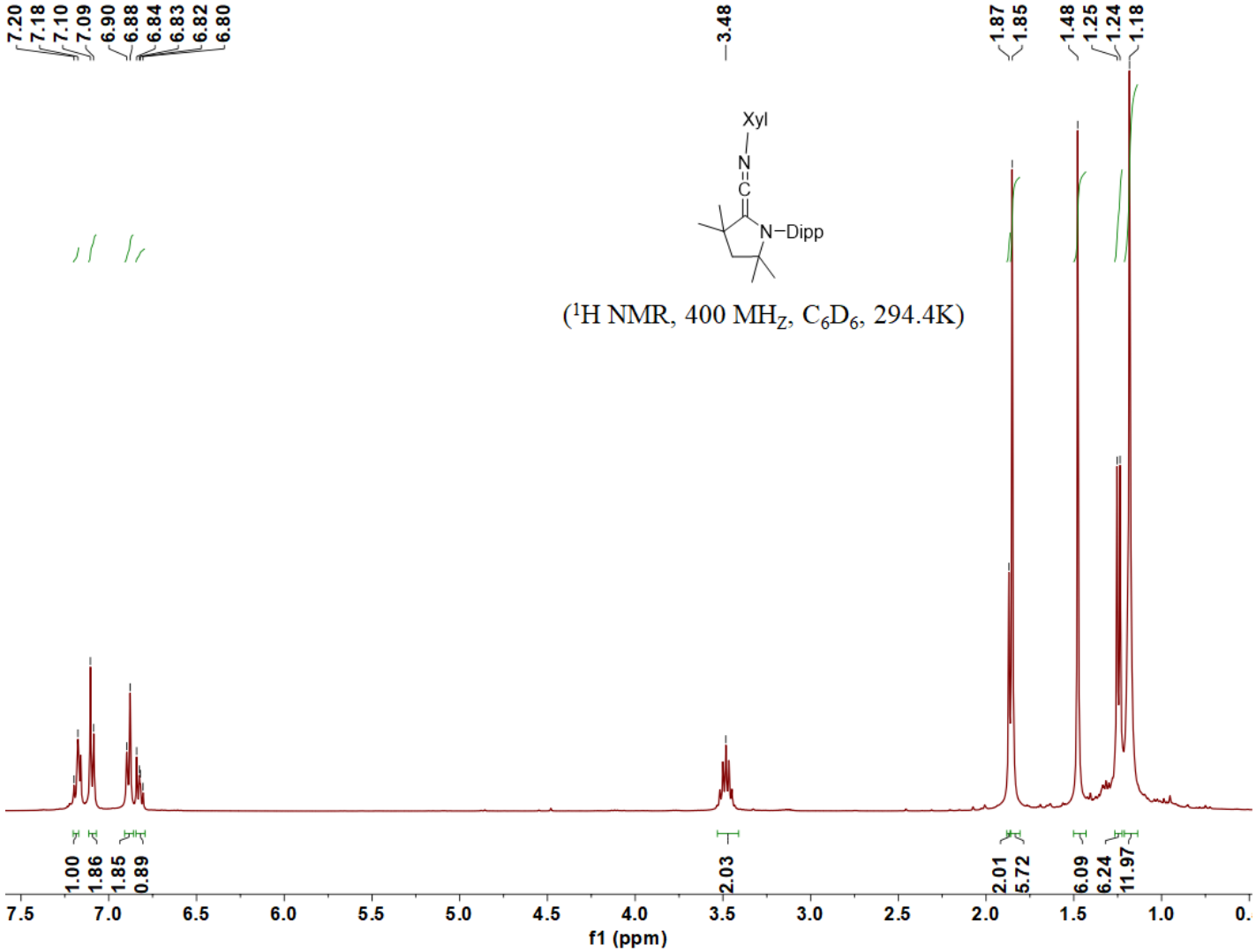

Figure S23. ^{1}H NMR spectrum for **8.**

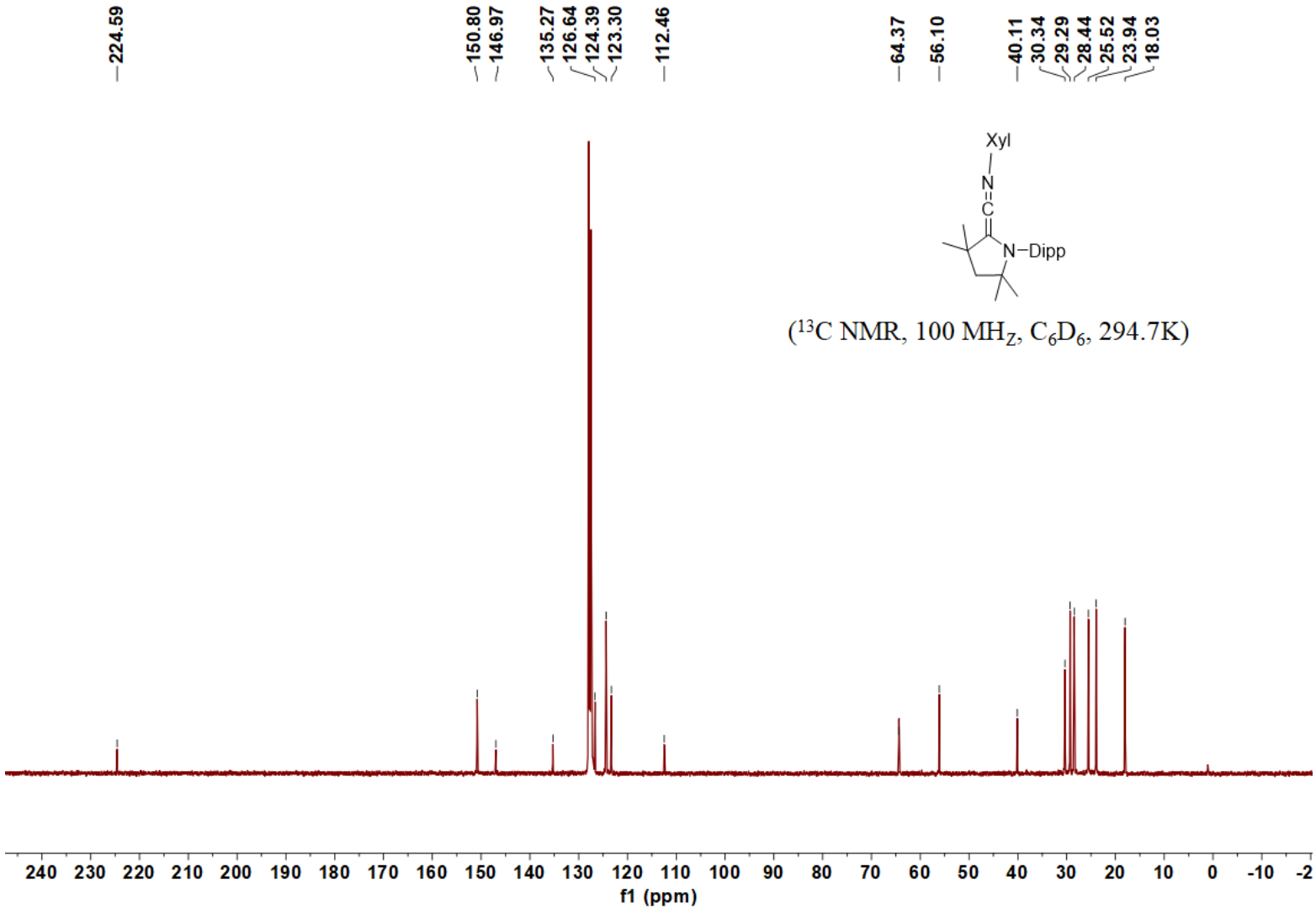

Figure S24. ^{13}C NMR spectrum for **8**.

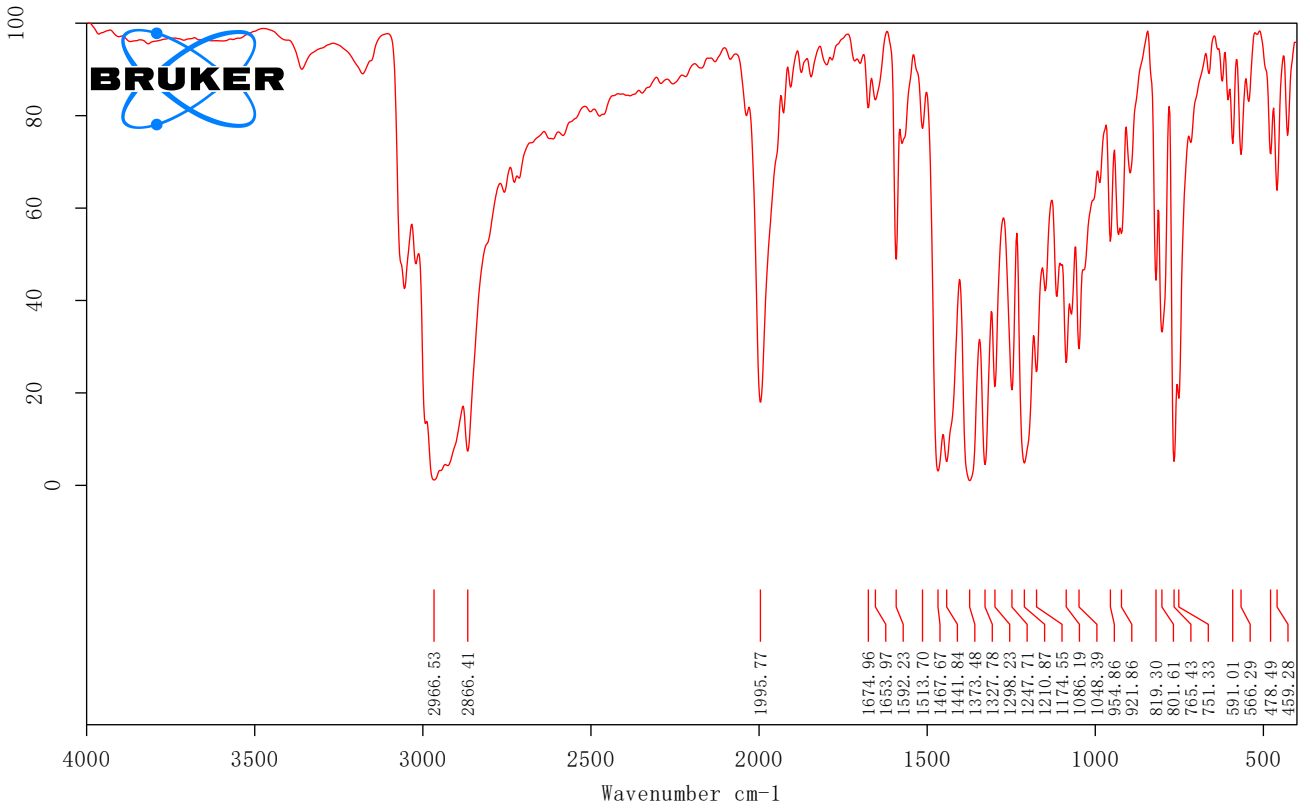

Figure S25. IR spectrum for **8**.

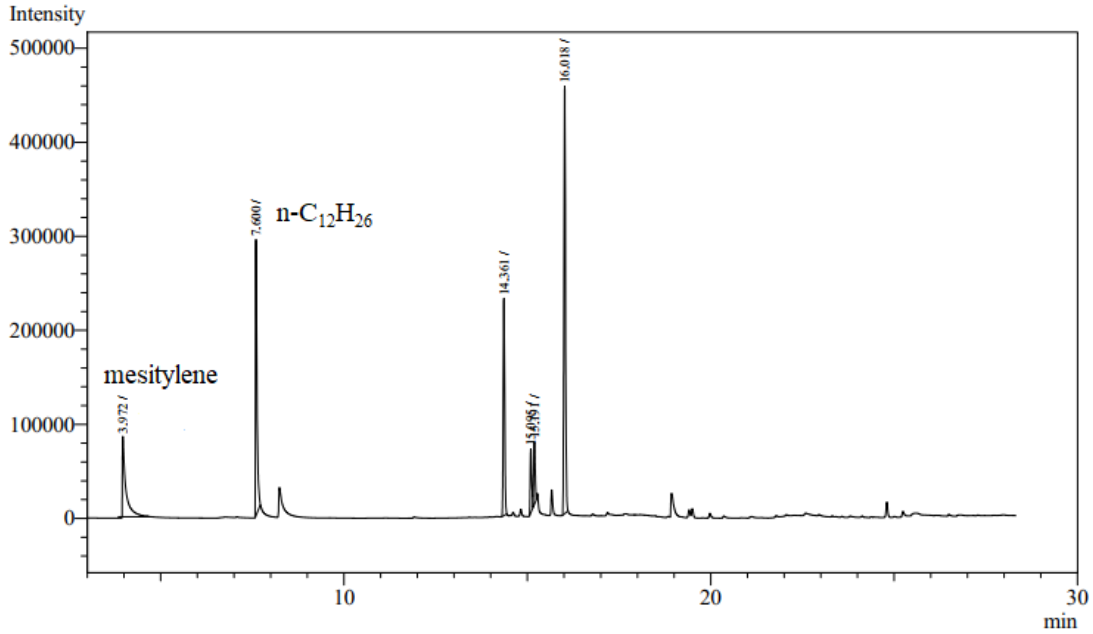

Figure S26. GC spectrum of the mixture formed from the reaction of **2** with MesBr in THF at room temperture after 12 hours.

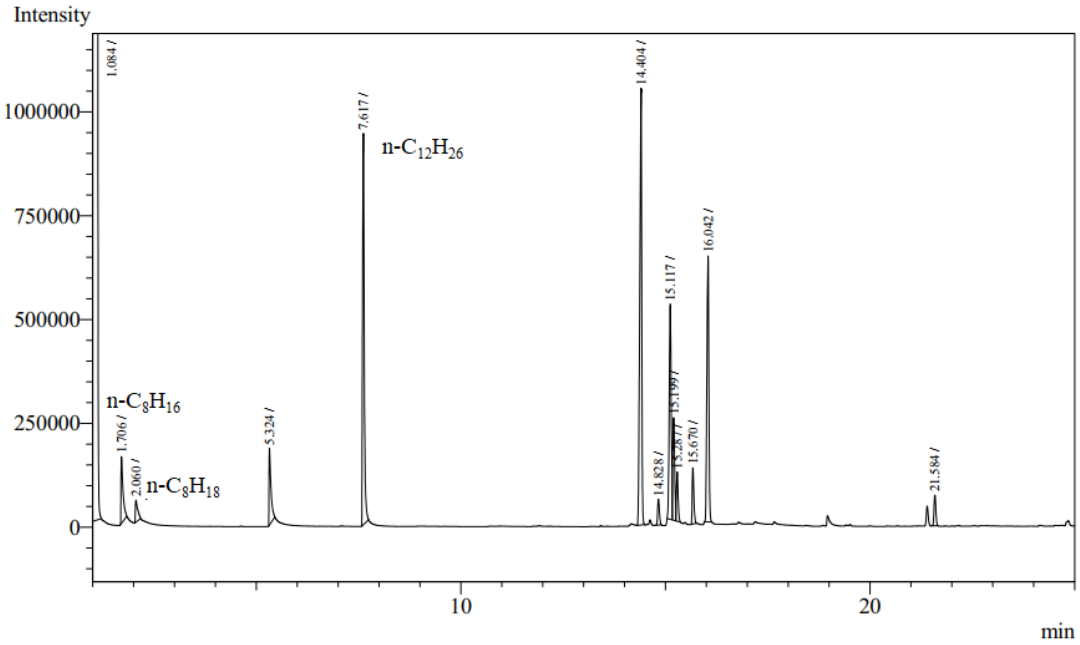

Figure S27. GC spectrum of the mixture formed from the reaction of **2** with n-$C_8H_{17}Cl$ in THF at room temperture after 12 hours.

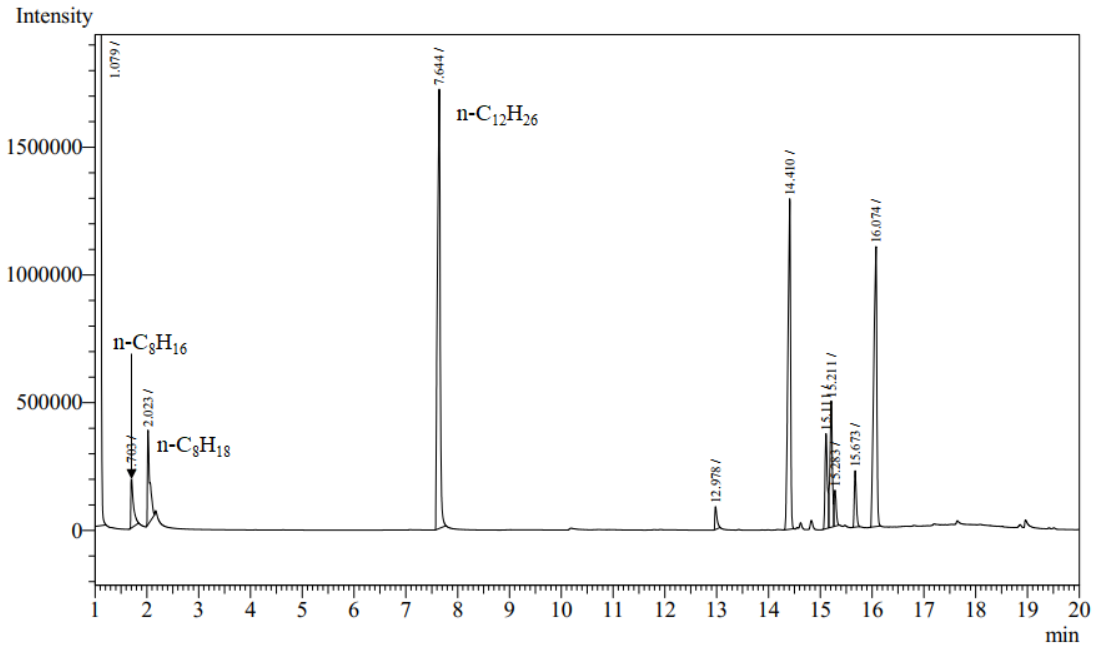

Figure S28. GC spectrum of the mixture formed from the reaction of **2** with n-$C_8H_{17}Br$ in THF at room temperture after 12 hours.

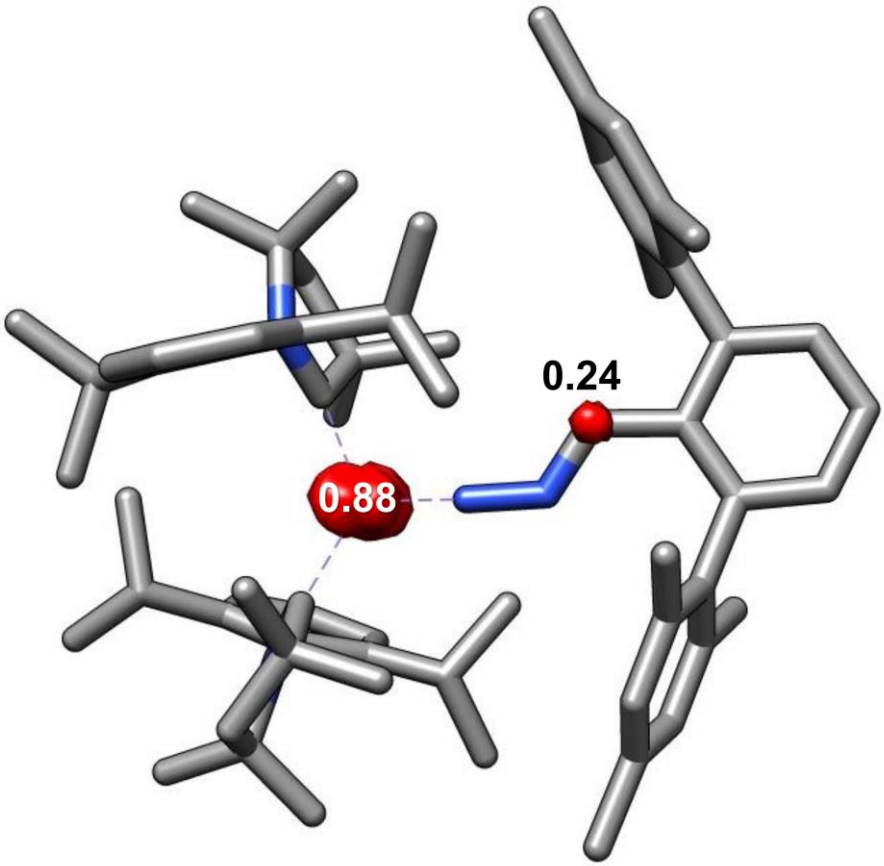

Figure S29. Mulliken spin populations of **6** (S = 1/2). The distribution of spin density: 0.88 in Co and 0.24 in C.

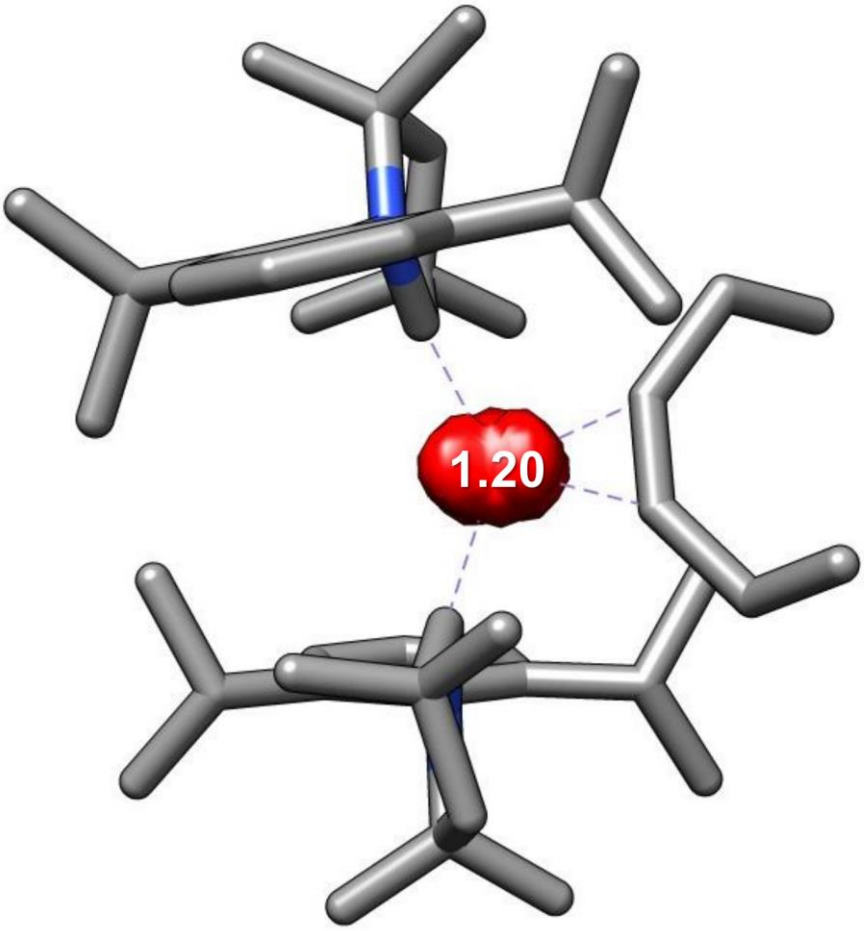

Figure S30. Mulliken spin populations of **9** (S = 1/2). The distribution of spin density: 1.20 in Co.

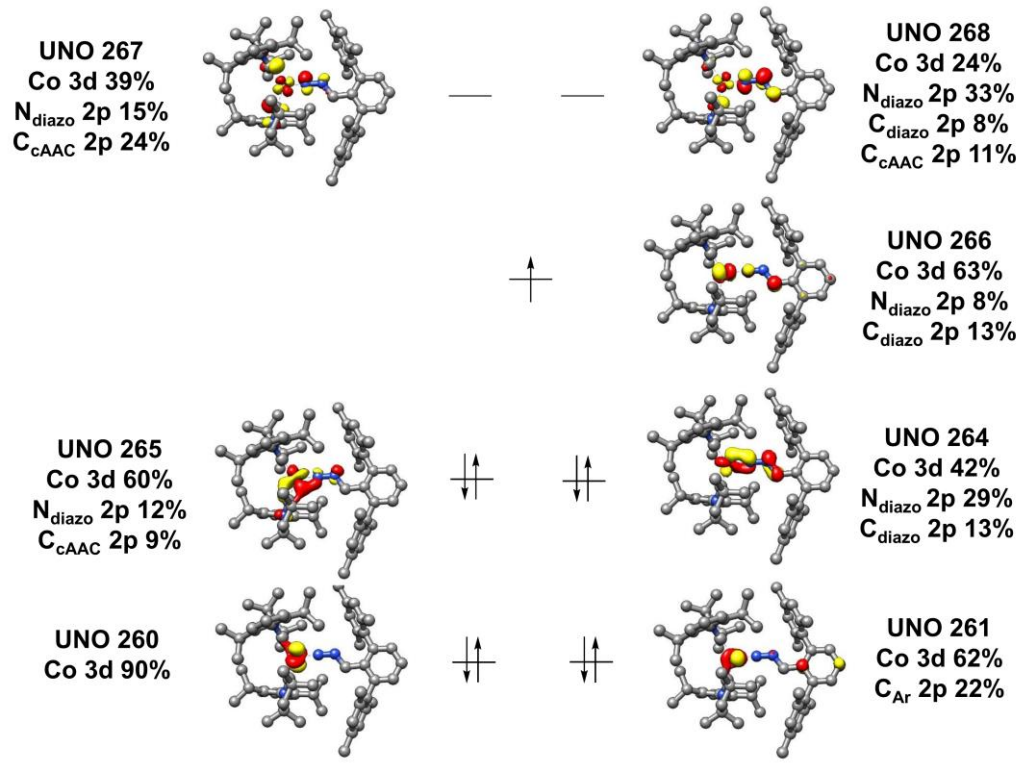

Figure S31. UNOs of **6** (S = 1/2).

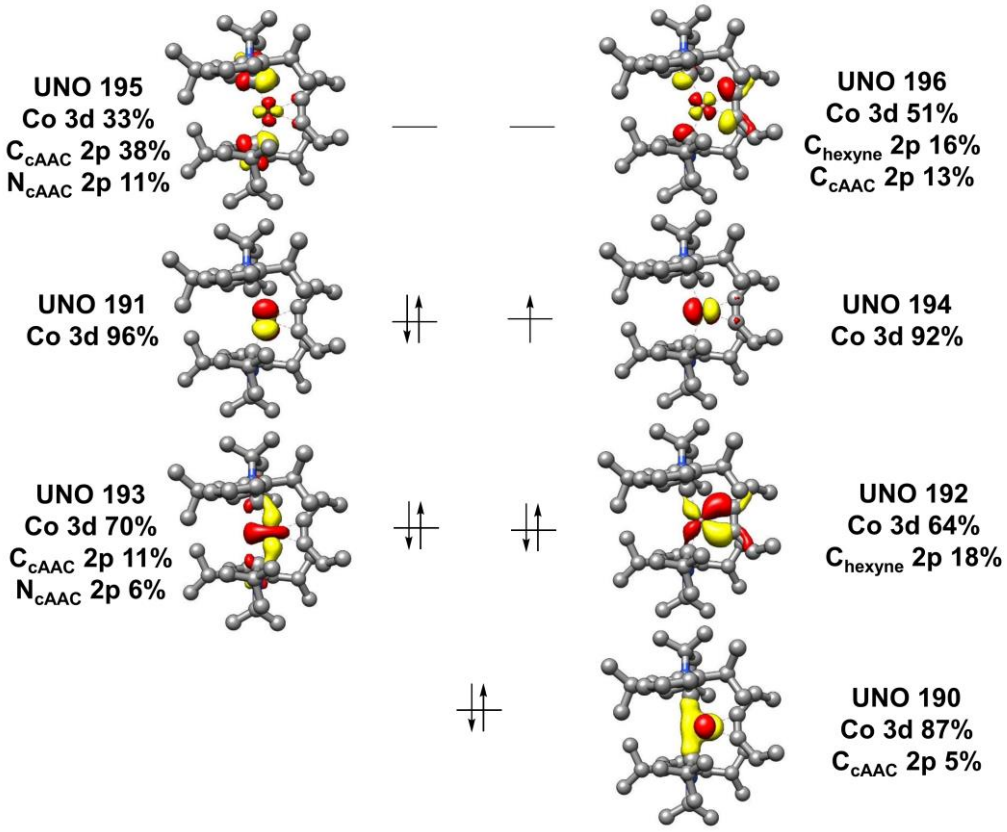

Figure S32. UNOs of **9** (S = 1/2).